ENVIRONMENTAL RESEARCH
ECOLOGY

Evaluation of isoprene light response curves for bryophyte-dominated ecosystems and implications for atmospheric composition

Ben Langford[1,*] ⓘ, James M Cash[3] ⓘ, Massimo Vieno[1] ⓘ, Mathew R Heal[2] ⓘ, Julia Drewer[1] ⓘ, Matthew R Jones[1], Sarah R Leeson[1], Ivan Simmons[1], Christine F Braban[1] ⓘ and Eiko Nemitz[1] ⓘ

1   UK Centre for Ecology and Hydrology, Edinburgh Research Station, Bush Estate, Penicuik EH26 0QB, United Kingdom
2   School of Chemistry, University of Edinburgh, David Brewster Road, Edinburgh EH9 3FJ, United Kingdom
3   The James Hutton Institute, Craigiebuckler, Aberdeen AB15 8QH, UK
*   Author to whom any correspondence should be addressed.

E-mail: benngf@ceh.ac.uk

Keywords: isoprene, ozone, bryophytes, eddy covariance

Abstract

Isoprene is emitted from numerous plant species in response to light and temperature and parameterisations of these relationships, based on observations from a few vascular plant species, have been shown to be broadly applicable to many different vegetation types. Here, we investigate their performance when applied to an ecosystem dominated by bryophytes. Over a six-week period, emissions of isoprene were measured above a Scottish peat bog. The light response derived on the basis of both canopy-scale flux and whole-plant enclosure measurements, deviated from the classical response, showing no sign of saturation within the observed range. We attribute this response to the canopy architecture of moss hummocks, which may attenuate light differently compared to a grass canopy. Both existing big-leaf and canopy-level emission algorithms, developed for vascular plants but commonly used for moorland vegetation, failed to replicate the observed fluxes, overestimating at low light intensities ($<1000\ \mu$mol m^{-2} s^{-1} photosynthetically active radiation) and underestimating during daytime clear sky conditions. The light response was optimised for bryophyte-dominated ecosystems using measured fluxes and incorporated into the EMEP4UK chemical transport model and applied exclusively to moorland. The revised parameterisation resulted in a small reduction in the average annual isoprene emissions in the northern latitudes (5%), but peak isoprene emissions and concentrations increased by up to a factor of two. Yet, no significant change in average or maximum surface ozone concentrations was observed, reflecting that the northern latitudes are in a chemical regime that is strongly NO$_x$ limited, in part due to the spatial segregation with the urban sources of NO$_x$. We conclude that, the anticipated increase in isoprene emissions from the northern latitudes in response to climate change is unlikely to contribute towards ozone-related air quality issues, as long as NO$_x$ pollution does not increase. However, the non-saturating light response may be equally applicable to non-vascular plants elsewhere, including in the tropics.

1. Introduction

Northern latitudes are dominated by semi-natural vegetation including heathland, moorland and arctic tundra. Within these ecosystems, bryophyte communities, including liverworts, mosses, and hornworts, flourish, many of which have been shown to emit the C_5H_8 molecule isoprene. Isoprene is a volatile organic compound (VOC) emitted by numerous higher plants in response to light and temperature, but it is particularly prevalent in emissions from non-vascular plants such as mosses but also in ferns [1]. Isoprene

has a short atmospheric lifetime [2], reacting quickly with hydroxyl (OH), the principal oxidant in the troposphere. In the presence of nitrogen pollution (oxides of nitrogen, NO_x) and sunlight, the products of this reaction can quickly form ground-level ozone [3] which damages both natural vegetation and crops [4], deteriorates building materials [5] and is harmful to health [6]. In addition, isoprene can react further to produce lower volatility oxidation products. These gases can condense onto pre-existing aerosols adding mass and thus, emissions of isoprene indirectly influence both cloud formation and rainfall patterns [7].

Previous measurements of isoprene from bryophyte dominated ecosystems are limited [8–14], but provide some evidence that semi-natural vegetation in the northern latitudes is a significant source of isoprene to the atmosphere. It is, therefore, important to determine isoprene emission rates from these regions and to understand their impact on air quality, as a precursor to photochemical ozone, both now and into the future. Rapid changes in climate, as predicted by the Intergovernmental Panel on Climate Change (IPCC), could see isoprene emissions from these ecosystems increase exponentially in the short term, with recent studies suggesting an increase of over 240% with a 2 °C–3 °C warming [15].

Isoprene emissions are routinely modelled from vegetation based on parameterisations of the emissions to changes in light (or photosynthesis), temperature, moisture and CO_2 [16–18] (G93). Yet, the reliability of the most widely used Guenther emissions algorithms [18–21] for predicting emission rates from ecosystems dominated by bryophytes is uncertain, because the light and temperature response curves used are based upon relationships established in higher vascular plants and plant canopies [18]. Bryophytes have developed numerous physiological (including morphology and structure) and biochemical adaptations since diverging from vascular plants [22] which mean there may be fundamental differences in how isoprene emissions from these species respond to environmental conditions. For example, as well as light and temperature, isoprene emissions from bryophytes are known to also be influenced by exposure to ultraviolet B radiation [9, 11, 12], sex [23], nutrient loading [23], ozone exposure [11] and water availability [8, 9, 13]. In addition, mosses have phyllids rather than true leaves and their canopy architecture differs from that of vascular plants; these differences are not represented in the Guenther algorithms.

Here we present the first set of ecosystem-scale isoprene flux measurements from an ombrotrophic peatbog in combination with whole-plant enclosure measurements taken from the dominant moss species present at the site. We use these new data to evaluate the performance of traditional isoprene emission algorithms and, in particular, to assess the light and temperature response of mosses at both the canopy- and the individual plant level. Using this information, we optimise the light response curves in the Guenther algorithms for use in predicting emissions from bryophyte-rich moorland vegetation and incorporate these changes into the EMEP4UK chemistry and transport model (CTM). We subsequently evaluate the extent to which isoprene emissions from semi-natural vegetation affect atmospheric composition and tropospheric ozone over Europe.

2. Method

2.1. Site description

Eddy covariance flux measurements of isoprene were made between the 8 June and the 21 July 2015 at the Auchencorth Moss (55°;47′32.4″N, 3°14′35.3″W, 270 m above sea level) European Monitoring and Evaluation Programme (EMEP) supersite. Auchencorth is an ombrotrophic peatbog situated 4.4 km south–west of the town of Penicuik, Scotland, and can be classified as a transitional lowland raised bog. The site comprises a mixture of peatland (85%) and grassland and covers an area of 5612 km², with an unobstructed fetch in the predominant wind sectors to the SW and NE [24]. The vegetation is dominated by coarse graminoids including *Eriophorum vaginatum, Molinia caerulea, Eriophorum angustifolium*, and *Deschampsia flexuosa*. In the wetter regions *Juncus effuses* is prevalent, and *Calluna vulgaris* is found in drier patches [24]. Mosses are widespread, with *Sphagnum* species quite common including *capillifolium, fallax* and *pallustre*, interspersed with *Pleurozium schreberi, Rhytidiadelphus squarrosus, Hylocomium splendens, Polytrichum commune* and *Polytrichum strictum*. Detailed site descriptions can be found in Drewer *et al* [25] and Dinsmore *et al* [26].

2.2. Flux measurements

Eddy covariance flux measurements were made using a high sensitivity quadrupole proton transfer reaction mass spectrometer (PTR-MS, IONICON Analytik GmbH, Austria) following a similar approach as Langford *et al* [27]. Sample air was drawn along a heated (30 °C), 15 m length of 1/4″ O.D. (I.D. 4 mm) perfluoroalkoxy (PFA) tubing at a rate of ~10 l min⁻¹. This flow rate ensured a turbulent flow was maintained (RE ≈ 3800) to limit the attenuation of VOC signals within the sample line. The inlet of the tube was positioned 5 cm below an ultrasonic anemometer (Windmaster Pro, Gill Instruments, Lymington, UK)

which measured the vertical wind velocity from a height of 3.1 m above the ground. The operating conditions of the PTR-MS were held constant throughout the measurement period to maintain a ratio between the electric field (E) to number density of molecules in the drift tube (N) of 110 Td. To achieve this, the drift tube pressure, voltage and temperature were set to 196 Pa, 450 V and 331 K, respectively. The primary ion (H_3O^+) minor isotopologue at *m/z* 21 and the first water cluster (*m/z* 37) were both measured by the PTR-MS alongside two VOCs, isoprene (*m/z* 69) and methanol (*m/z* 33, not discussed further), each at a rate of 5 Hz with a total duty cycle of 0.8 s. A LabVIEW (National Instruments, Austin, TX) program was used to alternate the acquisition mode between flux measurements (25 min), mass scan mode (21–146 *m/z*, dwell time 0.1 s, 5 min) and the instrument background (5 min). VOC-free air was supplied via a zero-air generator (model GC-1500, Linde gas, Dublin, Ireland) which removed VOCs by passing air through a heated (250 °C) platinum/palladium catalyst. This measurement protocol generated two 25 min flux averaging periods per hour together with an associated instrument background which was subtracted from the measured VOC concentrations.

Isoprene measurements made by the PTR-MS were calibrated against a gas standard (±5%, Ionicon, GmbH, Austria) at the start (9 June 2015) and at the end of the measurement period (15 July 2015). The standard which contained ∼1 ppmv of isoprene was diluted with VOC-free air to give a three-point calibration in the range of 0–20 ppb. The average instrument sensitivity from the two calibrations was 2.6 ncps ppb^{-1} and was applied across the entire measurement period.

Fluxes were calculated using equation (1) following a two-dimensional rotation of the coordinate frame to ensure the average vertical wind velocity ($\bar{w}$) was equal to zero:

$$F_\chi(\Delta t) = \frac{1}{N} \sum_{i=0}^{N} w'\left(i - \frac{\Delta t}{\Delta t_w}\right) \chi'(i). \tag{1}$$

Here, w' and χ' represent the instantaneous fluctuations of the vertical wind velocity (w) and isoprene concentration (χ), respectively. Δt represents the time delay between the air being measured by the ultrasonic anemometer and its subsequent analysis by the PTR-MS and Δt_w, is the sampling interval between wind measurements. Fluxes were initially calculated by searching for a maximum in the cross covariance function in each averaging period. The results were subsequently filtered to remove data where the flux was <200 μg m^{-2} h^{-1}. This process eliminated fluxes where the signal-to-noise ratio was low and allowed a frequency distribution of time-lags to be generated, which clearly indicated a value of 2.6 for Δt. Following the recommendations of Langford *et al* [28], the entire data set was subsequently re-processed using a prescribed time-lag of 2.6 s to eliminate possible systematic bias introduced by constantly searching for a maximum in the covariance function.

For each averaging period the random flux error (RE) was calculated using a method of Langford *et al* [28] which uses the statistical properties of the cross-covariance function, and these estimates are shown as error bars in the reported measured fluxes.

Additional quality assessments were applied to the data, including corrections for high frequency losses and a stationarity test. These are described in detail by Langford *et al* [29]. In total only 3% of the measured data were rejected based on non-stationarities. Fluxes measured during periods of low turbulence were retained as removing them causes the average diurnal pattern to be biased high, particularly at night.

2.3. Gas exchange measurements

2.3.1. Whole-plant enclosure measurements

Thirty-two moss samples from eight different species were collected from Auchencorth on the 23 November 2015. The mosses were placed in pre-weighed pots which were seated in 2 cm of water and left in an open unheated glasshouse. All plant species were left for a minimum of two weeks before testing began which has been shown to be a sufficient amount of time for plants to acclimatise and produce isoprene levels that reflect their growing conditions [30]. Meteorological data were collected throughout this period to provide a history of growth conditions since sample collection.

The laboratory emission measurements took place during the winter months of 2015 (December–February) and were repeated in spring (March–May). Moss samples were measured using a custom-built, whole-plant chamber with fixtures and fittings from a LI-6400-17 Whole Plant Arabidopsis unit (exposed ground surface area of 27 cm^2). The concentrations of CO_2 and H_2O, photosynthetically active radiation (PAR) and air flow were controlled and monitored using an infrared gas analyser (model Li-6400XT, Licor, Lincoln, Nebraska, USA). A Zero Air Generator (model GC 1500, Linde gas, Dublin, Ireland) was used to supply the chamber with VOC-free air and the concentration of isoprene was measured

at the chamber inlet (χ_1) and outlet (χ_2) using the same PTR-MS described above and with settings kept consistent with those used for the canopy flux measurements (see section 2.2).

The enclosure approach relies on an isolated flux chamber with a fixed volumetric flow of air Q, that is passed through the chamber. The concentration of the species of interest, χ combined with the ground surface area, s, can be used to calculate the flux F_χ as:

$$F_\chi = \frac{Q(\chi_2 - \chi_1)}{S}.$$ (2)

Corrections for the effect of evapotranspiration were not applied as they were typically below 1%.

2.3.2. Light and temperature ramps
The light and temperature response of the eight moss species was evaluated following a procedure similar to that described by Rasulov *et al* [31]. Each species was initially placed in conditions of 20 °C, 1000 μmol m^{-2} s^{-1} PAR and 400 μmol mol^{-1} of CO_2 at a flow rate of 500 μmol air s^{-1} to obtain an emissions rate for these standard conditions. Once a stable emission rate was established, the conditions were changed in set increments of either temperature or PAR and all other conditions were kept constant. The standard conditions were then reintroduced between each increment to quantify any deviation from the base emission rate which may indicate stress or a physiological change to the plant. The standard temperature of 30 °C typically used in the G93 model was not applied here because the highest temperature recorded at Auchencorth Moss in 2015 was 26.7 °C, and an emissions output at 30 °C may have caused thermal stress to the mosses, reducing their physiological activity [32].
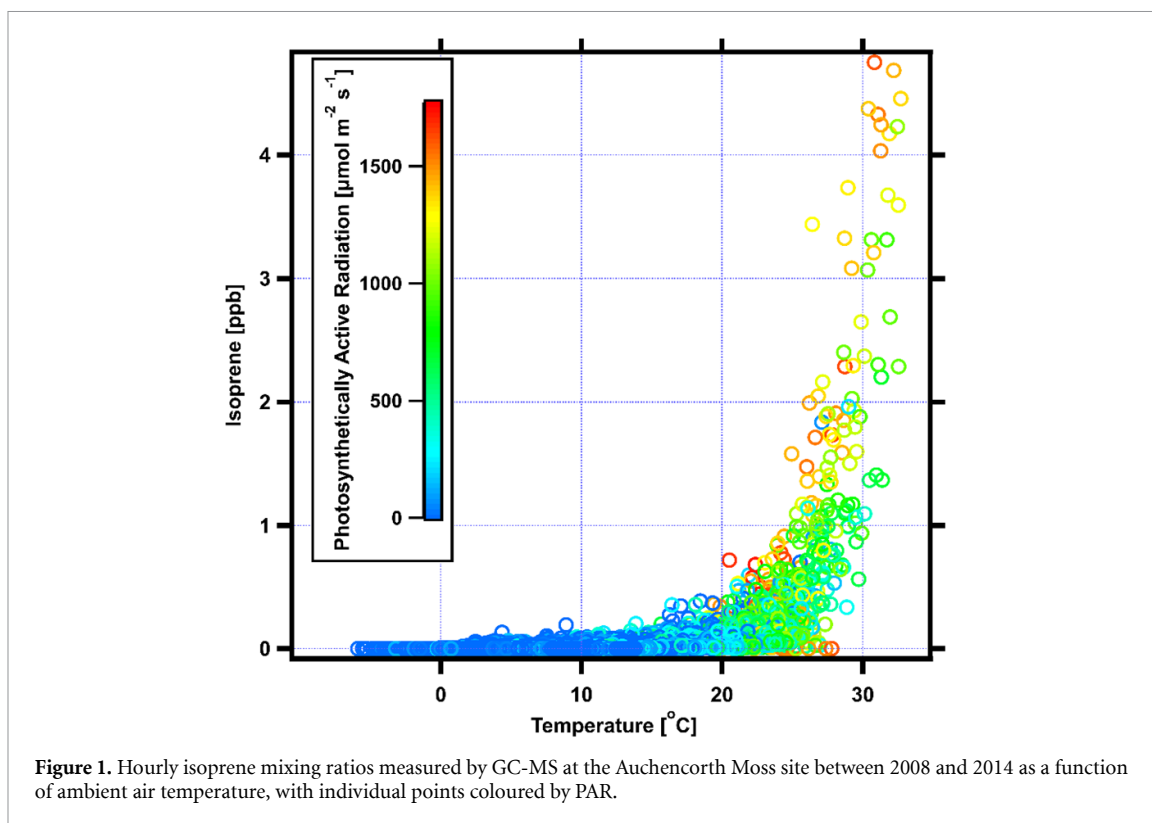
2.4. Isoprene emission algorithms
The time series of observed isoprene emissions from Auchencorth Moss was simulated using two versions of the isoprene emission algorithms developed by Guenther *et al* [21, 33], commonly used in CTMs for all vegetation types including those dominated by non-vascular plants, for comparison with the observed eddy-covariance flux measurements. The first (G93) is a simple emission algorithm that describes the response of an individual leaf to changes in light and temperature. While the algorithm was designed by Guenther *et al* [18], to be specifically applied to emissions from individual leaves, it is routinely used in CTMs (e.g. EMEP4UK-WRF) to model emissions from specific land classifications. Within these models, air temperature is assumed equivalent to the average leaf temperature and canopy-scale or branch-level emission potentials are used. It is in this context that the algorithm is used and evaluated within this study.

The second is the model of emissions of gases and aerosols from nature (MEGAN) which describes canopy-scale response to light and temperature but also to ambient CO_2, water availability and various other environmental parameters. Here, a detailed canopy environment (CE) model is used to parameterise the attenuation of light and temperature through the canopy and also accounts for the fraction of young, mature and old leaves which have differing emission potentials. MEGAN also considers the effect of previous meteorological conditions, incorporating changes in light and temperature over the previous 10 d. For this study, we ran the version of Pocket MEGAN (EXCEL, beta3) which was initialised with the ambient measurements of light and temperature and was setup for the 'cool C3 grasses' canopy type. CO_2 was held constant at 400 ppm, the leaf area index was set at 1.9 m^2 m^{-2} and the soil moisture algorithm was not used due to a lack in observations.

2.5. The EMEP4UK chemical transport model
The European Monitoring and Evaluation Programme Meteorological Synthesizing Centre-West (EMEP MSC-W) rv4.34 atmospheric chemistry transport model has been developed by the EMEP MSC-W. As described by Simpson *et al* [34]. The EMEP MSC-W model application used here is named EMEP4UK-WRF. The model uses 21 layers of hybrid terrain-following vertical coordinates, with the top of the vertical column set at 100 hPa ($\sim$16 km) and the surface layer has a thickness of about 45 m. The EMEP4UK-WRF model domain covers Europe with a horizontal resolution of 27 $\times$ 27 km^2. The EMEP4UK-WRF model meteorological driver used for this study is the Weather Research and Forecast (WRF) model WRF version 4.2.2 [35]. A detailed description of the EMEP4UK-WRF model is given in Vieno *et al* [36, 37] and in Ge *et al* [38]. The EMEP model used here calculates isoprene emissions using the G93 emission algorithm, adopting a simple non-canopy approach that assumes air temperature is similar to the average leaf temperature [34]. In addition, to account for the effects of shading the algorithm uses branch-level emission potentials, which are typically a factor of 1.75 smaller than leaf-level values [39]. The model has been updated with the newly derived algorithm for the isoprene emissions from this study.
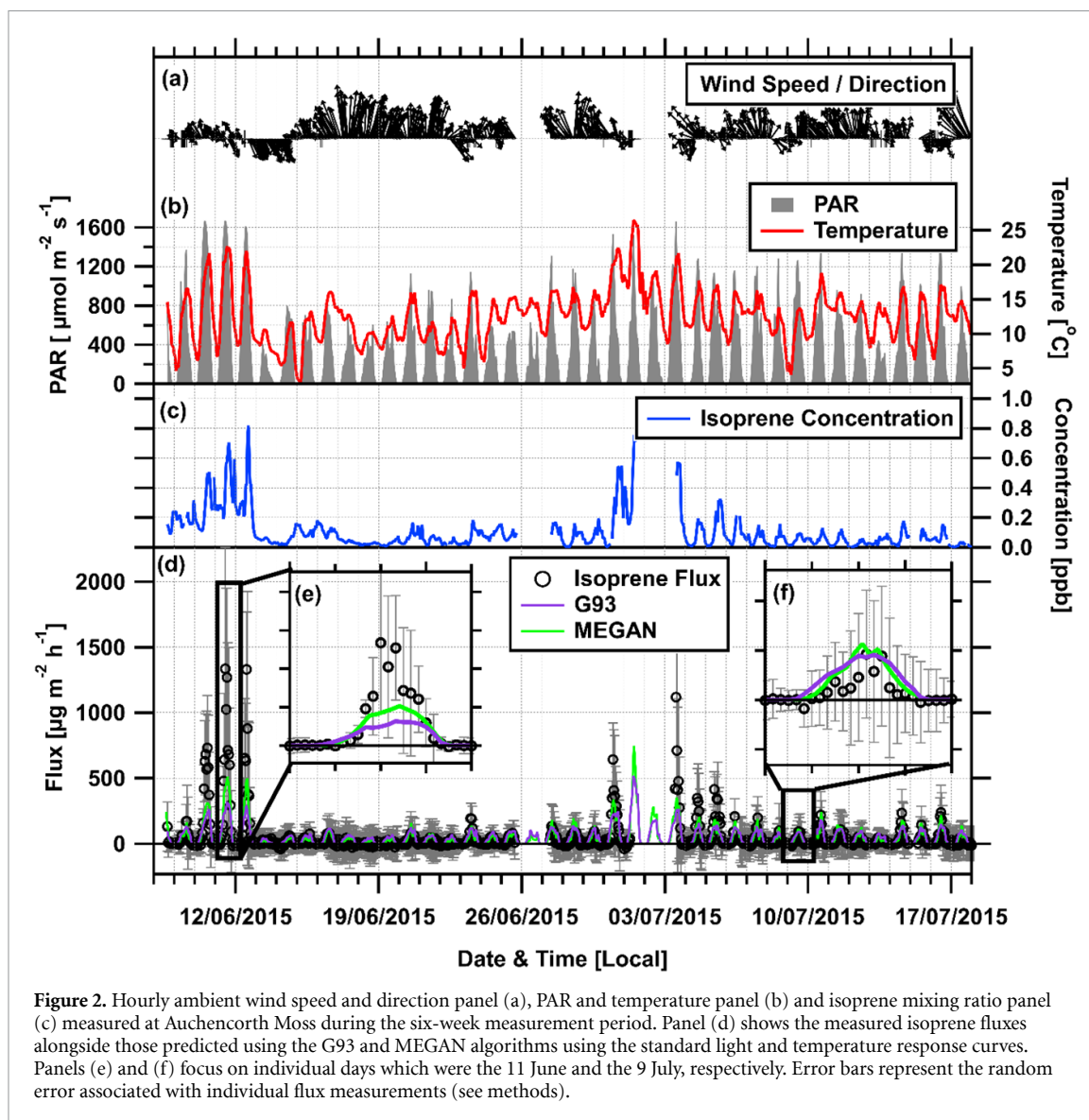
Figure 1. Hourly isoprene mixing ratios measured by GC-MS at the Auchencorth Moss site between 2008 and 2014 as a function of ambient air temperature, with individual points coloured by PAR.

3. Results and discussion

3.1. Field measurements

Observations of hourly ambient isoprene mixing ratios have been made at the Auchencorth Moss site since 2006 as part of the UK Automatic Hydrocarbon Network, ratified QA/QC data is available at the UK-Air website (https://uk-air.defra.gov.uk/data/). As shown in figure 1, mixing ratios are typically below 0.25 ppb but increase rapidly as the temperature passes 20 °C to a maximum of >4 ppb at 30 °C and 1500 μmol m^{-2} s^{-1} of PAR. These measurements, made by gas chromatography mass spectrometry (GC-MS), demonstrate that the association of elevated isoprene concentrations with warm temperatures is a general characteristic of the site and also provide assurances for our study, that the signal measured at *m/z* 69 in the PTR-MS is likely to be isoprene rather than a fragment of methyl-3-buten-2-ol which would also be detected at this unit mass.

Figure 2 shows the variation in wind speed and direction (a), light and temperature (b), as well as the ambient isoprene mixing ratio (c) and emission flux (d) measured during the six-week sampling period at Auchencorth Moss. During this period the typical midday (10:00–14:00) temperature was 15 °C and PAR was 780 μmol m^{-2} s^{-1}. Mixing ratios of isoprene remained below 1 ppb during the 6 weeks of measurements with an average of 0.12 ppb. During the warmer periods, which were associated with lower wind speeds, isoprene mixing ratios remained elevated throughout the night, whereas more typically, and especially under higher wind speeds, they dropped to zero. This relates to the shutoff of the isoprene source at night and the rapid transport of the daytime emissions away from the site under more turbulent conditions. Emissions of isoprene typically peaked between 100–200 μg m^{-2} h^{-1}. However, two short spells of warmer weather provided a few days on which temperatures exceeded 20 °C and PAR increased to >1500 μmol m^{-2} s^{-1}. On these occasions isoprene emissions were enhanced, peaking between 700 and 1300 μg m^{-2} h^{-1}. Figure 2(d) shows the measured isoprene fluxes along with those predicted by both the simple G93 emission algorithm (purple) and the more advanced MEGAN model which uses the CE model (green). As described in section 2.4, the emission potential used for each algorithm was first calculated following the methods outlined by Langford *et al* [40]. Using the weighted average method to calculate the emission potential ensures that the modelled fluxes have the same average flux as the observations, but it is clear that the distribution of the flux across the day does not closely follow that of the observations. This is particularly apparent on the 11 June (figure 2(e)), where modelled midday fluxes are approximately half of

Figure 2. Hourly ambient wind speed and direction panel (a), PAR and temperature panel (b) and isoprene mixing ratio panel (c) measured at Auchencorth Moss during the six-week measurement period. Panel (d) shows the measured isoprene fluxes alongside those predicted using the G93 and MEGAN algorithms using the standard light and temperature response curves. Panels (e) and (f) focus on individual days which were the 11 June and the 9 July, respectively. Error bars represent the random error associated with individual flux measurements (see methods).

the measured emissions. By contrast, on the cooler days, such as the 9 July (figure 2(f)), the model tends to overestimate the emission flux across the day, especially in the morning period.
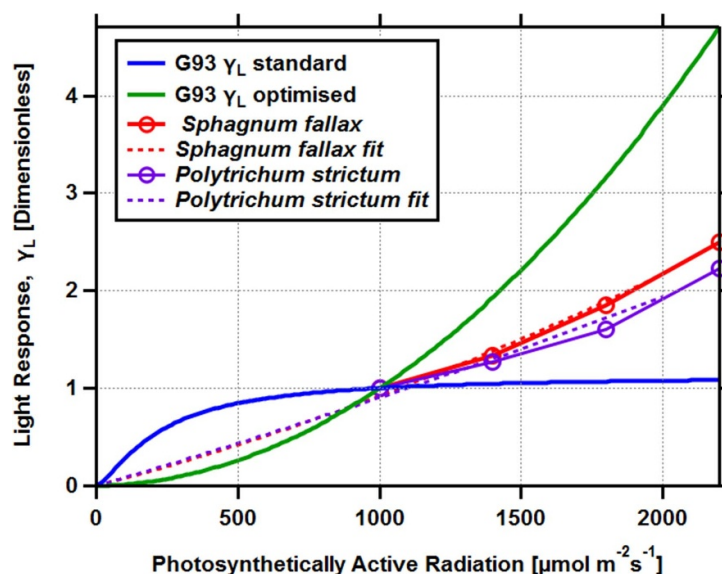
3.2. Whole-plant chamber measurements

3.2.1. Isoprene emission potentials

Table 1 lists the emission potentials of the individual moss species measured at (a) 26 °C and 1800 μmol m^{-2} s^{-1} PAR and (b) converted to standard conditions (30 °C and 1000 μmol m^{-2} s^{-1} PAR) using the G93 light and temperature response curves. Of the emission potentials of the eight species screened, three were identified to be non-emitters (*P. schreberi*, *H. splendens* and *Sphagnum pallustre*), two were relatively low emitters (<30 μg m^{-2} h^{-1}) (*Sphagnum capillifolium* and *Hypnum imponens*) and three showed much larger emission rates (>200 μg m^{-2} h^{-1}) (*P. commune*, *P. strictum* and *Sphagnum fallax*). The emission potentials of these mosses differed strongly between seasons, with values on average three times larger when measured in spring compared with winter under the same standard conditions. The measurements were made on a per ground area basis rather than per plant biomass or per leaf area, which means this change may reflect plant growth between seasons. A second, more credible argument is that during the winter months light intensity is reduced and temperatures frequently fall to below freezing. Sudden exposure to high light intensities may stress the moss causing photoinhibition of photosynthesis and ultimately a reduced isoprene emission potential. Photoinhibition can be further enhanced when plants are exposed to parallel stresses and in *S. fallax* for example, it has previously been linked to low tissue levels of nitrogen, often associated with this species [41]. The distribution of moss species at Auchencorth Moss is highly spatially variable, but *S. fallax* is thought to be the most prevalent *Sphagnum sp.* within the flux

Table 1. List of moss species present at Auchencorth Moss and their measured isoprene emission potential (e.g. the emission rate at 30 °C and 1000 μmol m^{-2} s^{-1} of PAR) in winter and spring.

Moss species	Emission potential at 1800 PAR and 26 °C (μg m^{-2} h^{-1}) (Winter)	Emission potential G93 at 1000 PAR and 30 °C (μg m^{-2} h^{-1}) (Winter)	Emission potential G93 optimised at 1000 PAR and 30 °C (μg m^{-2} h^{-1}) (Winter)	N	Emission potential at 1800 PAR and 26 °C (μg m^{-2} h^{-1}) (Spring)	Emission potential G93 at 1000 PAR and 30 °C (μg m^{-2} h^{-1}) (Spring)	Emission potential G93 optimised at 1000 PAR and 30 °C (μg m^{-2} h^{-1}) (Spring)	N	Literature emission potential (μg m^{-2} h^{-1})	Reference
P. schreberi	0	0	0	2	0	0	0	1	—	—
H. splendens	4 ± 3	6.1 ± 3	4 ± 3	2	35 ± 5	55 ± 5	38 ± 5	1	1	Hanson and Sharkey (1999)
P. commune	211 ± 72	324 ± 73	226 ± 73	3	634 ± 374	995 ± 381	681 ± 381	3	—	—
P. strictum	781 ± 87	1202 ± 88	838 ± 88	3	1994 ± 385	3071 ± 392	2140 ± 392	2	—	—
S. fallax [14]	0	0	0	2	483 ± 207	744 ± 211	518 ± 211	3	680	[14]
S. capillifolium	28 ± 15	43.0 ± 15	31 ± 15	2	94 ± 12	145 ± 12	101 ± 12	1	27	Hanson and Sharkey (1999)
S. pallustre	21 ± 20	32 ± 21	22 ± 21	2	0	0	0	1	—	—
H. imponens	13 ± 2	20 ± 2	15 ± 2	2	44 ± 7	68 ± 7	47 ± 7	1	—	—

Figure 3. Whole-plant isoprene light response curves for the mosses *S. fallax* (red) and *P. strictum* (purple) when measured in spring (solid) relative to the classical Guenther (G93) light response curve (blue) and the optimised light response curve (green) that best describes the ecosystem-level eddy covariance flux measurements at the Auchencorth Moss site. Dashed lines show an extrapolation of the *S. fallax* and *P. strictum* light response curves based on a three-point quadratic fit to the observations.

footprint of the eddy covariance measurements. The isoprene emission potential for *S. fallax* measured in the spring was 744 μg m^{-2} h^{-1}, whereas the average of all moss species screened in the laboratory was 619 μg m^{-2} h^{-1}. Without knowing the exact coverage of these species at our site and given the limitations of the chamber measurements, which did not explicitly account for plant biomass, extrapolating these measurements to give a representative emission potential for the site is not possible. However, the canopy-scale flux measurements can be used to work back to an emission potential by normalising the measurements to standard conditions using an emission algorithm as mentioned in section 3.1 and discussed in detail by Langford *et al* [40]. Using this approach does not require a detailed knowledge of the species present and will capture an emission potential that comprises emissions from both the screened bryophytes and vascular isoprene emitters such as *C. vulgaris* that were not assessed as part of the laboratory work.

    The isoprene emission potential for our site was found to be 769 μg m^{-2} h^{-1} when normalising using the standard light response curve and 1035 μg m^{-2} h^{-1} when using the light response curve optimised on the basis of the derived flux measurements. The default isoprene emission potential for moorland within the EMEP4UK model (where it is applied with the standard response curve) is 413 μg m^{-2} h^{-1} which was just over half that measured at Auchencorth. The MEGAN model uses plant functional types (PFTs) rather than land cover and, therefore, a specific emission potential for moorland is not included. The PFT that best describes the Auchencorth site is the 'cool C3 grasses' which have an emission potential of 800 μg m^{-2} h^{-1}. Optimisation against the measured data gave a new emission potential of 1930 μg m^{-2} h^{-1}.

3.2.2. Light response curves
Figure 3 shows the light response curves for the two most abundant isoprene emitting bryophyte species found at Auchencorth Moss, *S. fallax* and *P. strictum,* relative to the standard light response curve used in the G93 emission algorithm. Classically, the light response (originally derived for vascular plants) saturates above light intensities of 1000 μmol m^{-2} s^{-1} but neither species shows any sign of light saturation. Instead, they follow more closely the general trend of light response found to best describe canopy-scale flux measurements made at Auchencorth Moss. This deviation from the classical light response implies that isoprene emissions from landscapes dominated by these bryophyte species will be overestimated at light intensities below 1000 μmol m^{-2} s^{-1} and underestimated under clear sky conditions (>1000 μmol m^{-2} s^{-1}).

3.3. Canopy-scale light response
Figure 4 shows the average normalised canopy-scale light response curves derived from eddy covariance flux measurements made above tropical forests, including in Borneo [42] and the Amazon rainforest [43], and temperate forests in the UK, Italy, and France mixed oak forests [40]. When assessed relative to the classical light response curve of Guenther *et al* [18], each of these canopy-scale light response curves behaves in a similar pattern, showing a linear increase with light and saturation only evident for the sites with a larger leaf
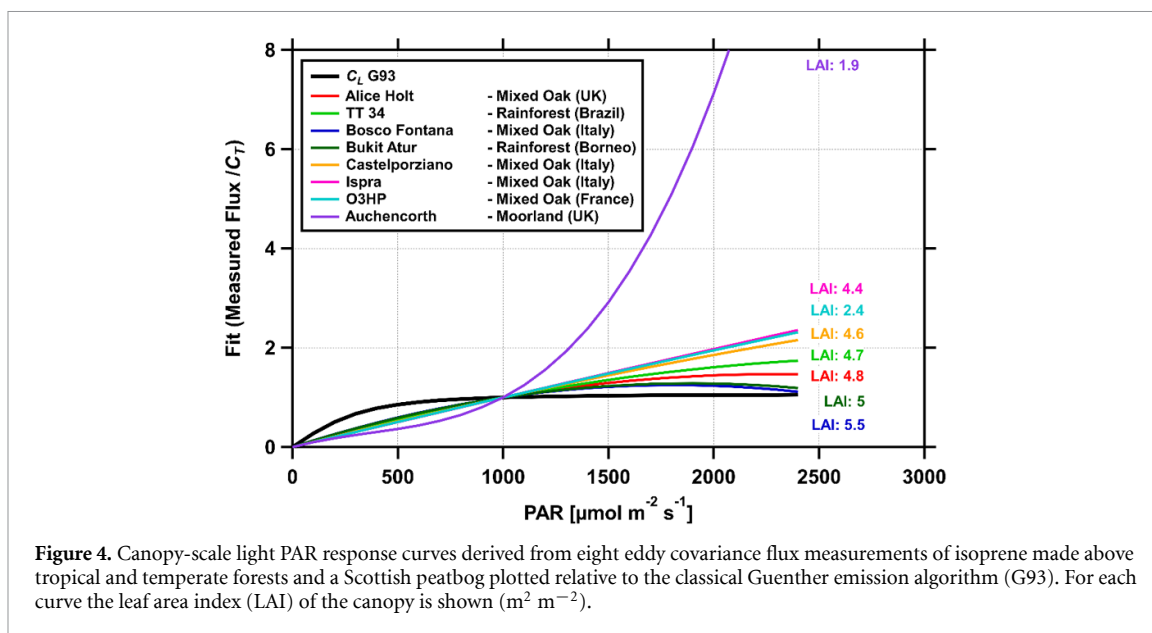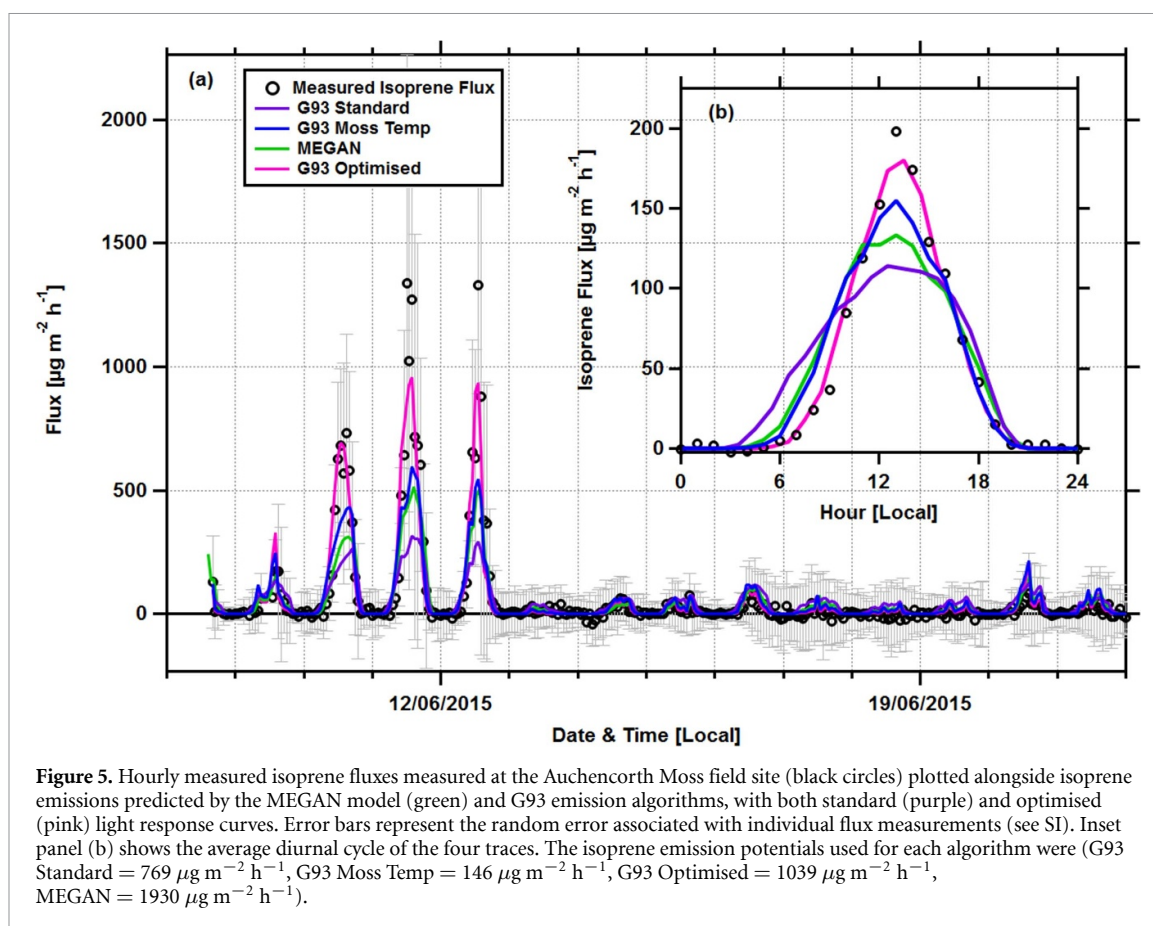
Figure 4. Canopy-scale light PAR response curves derived from eight eddy covariance flux measurements of isoprene made above tropical and temperate forests and a Scottish peatbog plotted relative to the classical Guenther emission algorithm (G93). For each curve the leaf area index (LAI) of the canopy is shown ($m^2\ m^{-2}$).

area index (>4.5). This deviation from the classical leaf-level response is expected as the flux measurements were made at the canopy-scale. By comparison, the light response observed in the canopy-scale flux measurements made at Auchencorth Moss is markedly different. Emissions increase exponentially with light, with no evidence of saturation. This observation is consistent with the individual plant-level light response curves for both *S. fallax* and *P. strictum* which show a similar, non-saturating pattern and indicates that these two species are likely to be the dominant source of isoprene emissions at this peatbog site.

There are two potential reasons for the remarkable light response observed at Auchencorth Moss. Firstly, as already mentioned, the G93 algorithm was developed to describe the isoprene emission from a single leaf, whereas here, it is applied to model the average canopy-scale response. At the canopy-scale, light is attenuated as it penetrates through the vegetation and, therefore, may cause the observed changes in response, with very little of the canopy actually receiving the full light intensity. Similarly, our light response curves measured in the laboratory were made at the whole-plant level and are, therefore, susceptible to the same attenuation of light through the moss' foliage. However, even when using the more recent MEGAN emission algorithm with detailed CE model [21], only a modest improvement in the model/measurements comparison was found, as shown in figure 5. This may reflect the fact that mosses, which form distinct clumps or hummocks, have a very different underlying canopy architecture than grassland, which means even a detailed CE model should not be expected to perform well for these ecosystems unless specifically designed for this canopy type. The second likely contributing factor at this specific site, where mosses of the *Polytrichum* genus are present, relates to plant physiology. Mosses non-vascular leaf equivalents, the phyllids, have specialised photosynthetic cells called lamella which are arranged in a comb-like (adaxial strands) structure which provides an increased area for CO_2 uptake and facilitates the use of direct sunlight [44]. However, the fact that we see non-saturating light curves not only for *P. strictum* but also for *S. fallax*, a species not known to have a similar lamella structure, points to canopy architecture as the most likely driver of this behaviour at this site.

The G93 algorithm, as implemented in the EMEP4UK model, assumes air temperature to be equivalent to that of the average leaf. In contrast, MEGAN converts air temperature to leaf surface temperature based on the radiation balance of a leaf. Air temperature typically increases at high light intensities and therefore, one possible explanation for the observed light response is that the moss surface temperature is significantly higher than the air temperature. Perera-Castro *et al* [45] developed an empirical relationship between photosynthetic photon flux density (PPFD) and surface temperature for three moss species (*Bryum pseudotriquetrum, Schistidium antarctici* and *Ceratodon purpureus*) at a site in Antarctica. Using this relationship the moss surface temperature at Auchencorth was estimated and used in a second run of the G93 algorithm. The emission potential based on the new temperature was calculated at 146 μg m^{-2} h^{-1}.

It should be noted, that the difference in air and moss temperature will vary with atmospheric turbulence and soil moisture availability and that the representativeness of the Perera-Castro *et al* [45] data for our field site is unknown. Although their work did not use the same moss species as found in our flux footprint, no difference in the energy balance of their three test species was found. Bearing in mind these uncertainties, when applied to the Auchencorth Moss data, the resulting moss surface temperatures were on average 12 °C higher than air temperature at midday. The resulting isoprene emissions were similar to those predicted by

Figure 5. Hourly measured isoprene fluxes measured at the Auchencorth Moss field site (black circles) plotted alongside isoprene emissions predicted by the MEGAN model (green) and G93 emission algorithms, with both standard (purple) and optimised (pink) light response curves. Error bars represent the random error associated with individual flux measurements (see SI). Inset panel (b) shows the average diurnal cycle of the four traces. The isoprene emission potentials used for each algorithm were (G93 Standard = 769 μg m^{-2} h^{-1}, G93 Moss Temp = 146 μg m^{-2} h^{-1}, G93 Optimised = 1039 μg m^{-2} h^{-1}, MEGAN = 1930 μg m^{-2} h^{-1}).

MEGAN, but still underestimated peak emissions while overestimating emissions at lower PAR. This implies that surface temperature is unlikely to account for the observed non-saturating light response.

The light response curve (C_L) shown in figure 4 could not be replicated through the optimisation of the coefficients in the G93 emission algorithm due to the exponential growth of the response, rather than the classical exponential rise to a maximum. Instead, and in lieu of a CE model optimised for a bryophyte canopy, we describe the canopy-scale light response using a simple second-order polynomial as follows

$$C_L = aL^2 + bL \qquad (3)$$

where L is PAR in μmol m^{-2} s^{-1}, and a (-1.9×10^{-7} m^4 s^2 μmol^{-2}) and b (1.2×10^{-3} m^2 s μmol^{-1}) are empirical coefficients.

As with the standard light response curve, the value of C_L is set to unity at standard conditions (e.g. 1000 μmol m^{-2} s^{-1} PAR). Figure 5 compares the performance of this new response curve when integrated into the G93 emission algorithm relative to both the standard (non-optimised) algorithm and the MEGAN model. When adopting the optimised, non-saturating light response, the modified G93 algorithm is now better able to replicate the peak emissions during the warmer periods. On an average basis the optimised algorithm very closely captures both the diurnal profile and peak emission rate.

The fact that the light-response curve derived from canopy-scale flux measurements is similar to that seen from individual plants in the laboratory suggests that (a) plants with a classical light-response curve (e.g. vascular plants) make a minor contribution to the isoprene emissions at Auchencorth Moss and (b) that the change of the solar zenith angle over the day has little impact on the diurnal cycle of emissions. Whilst the light always came from above in the laboratory investigations, in real world condition the solar zenith angle changes and this is usually taken into account, e.g. in the full CE model that forms part of MEGAN. For moss the solar zenith angle appears to have little effect on light penetration into the canopy.

Having established that the emission algorithm can reliably replicate the measurements at this site, we incorporated the new light response curve into the EMEP4UK chemical transport model to allow us to model isoprene emissions from the northern latitudes of Europe.
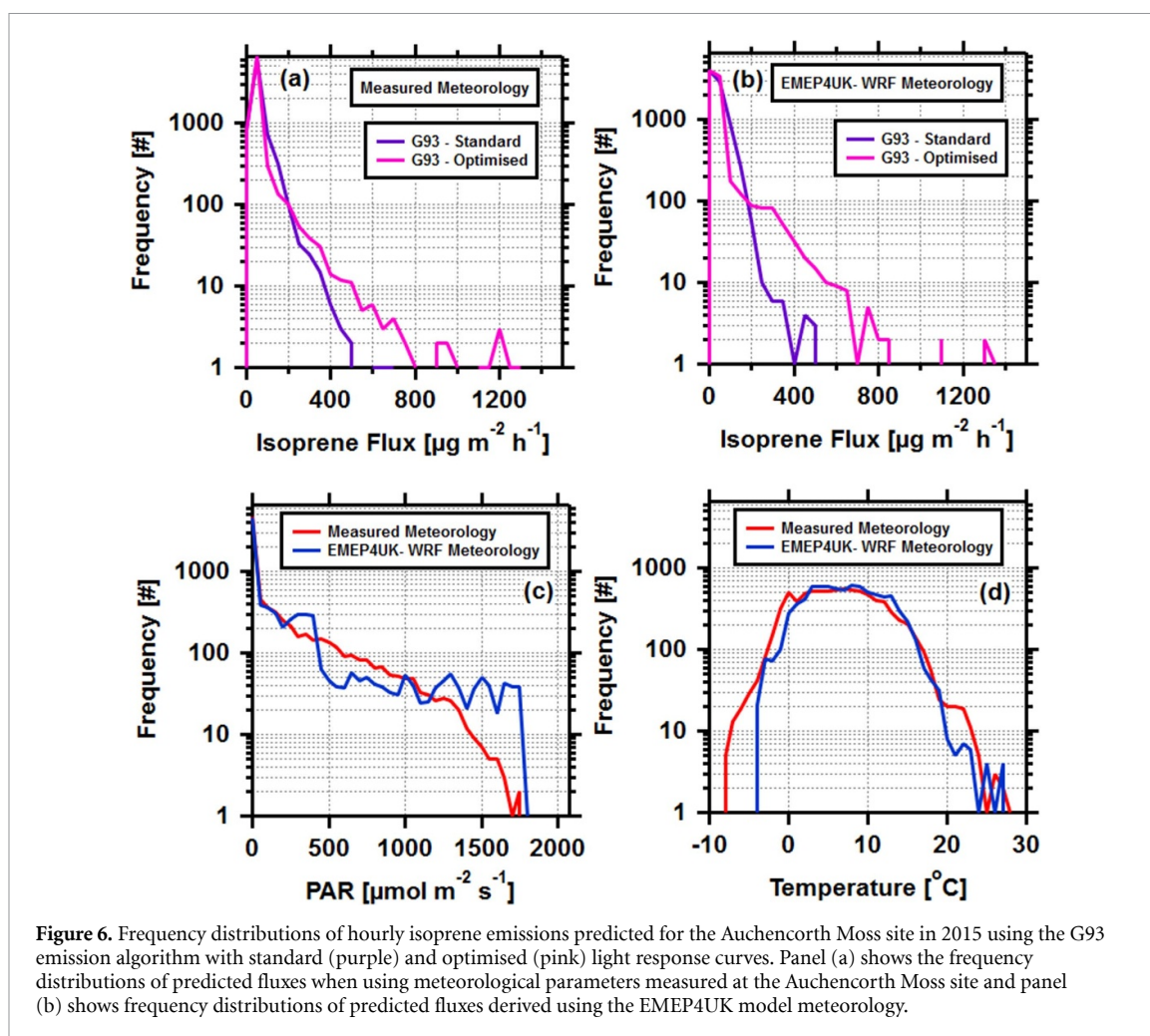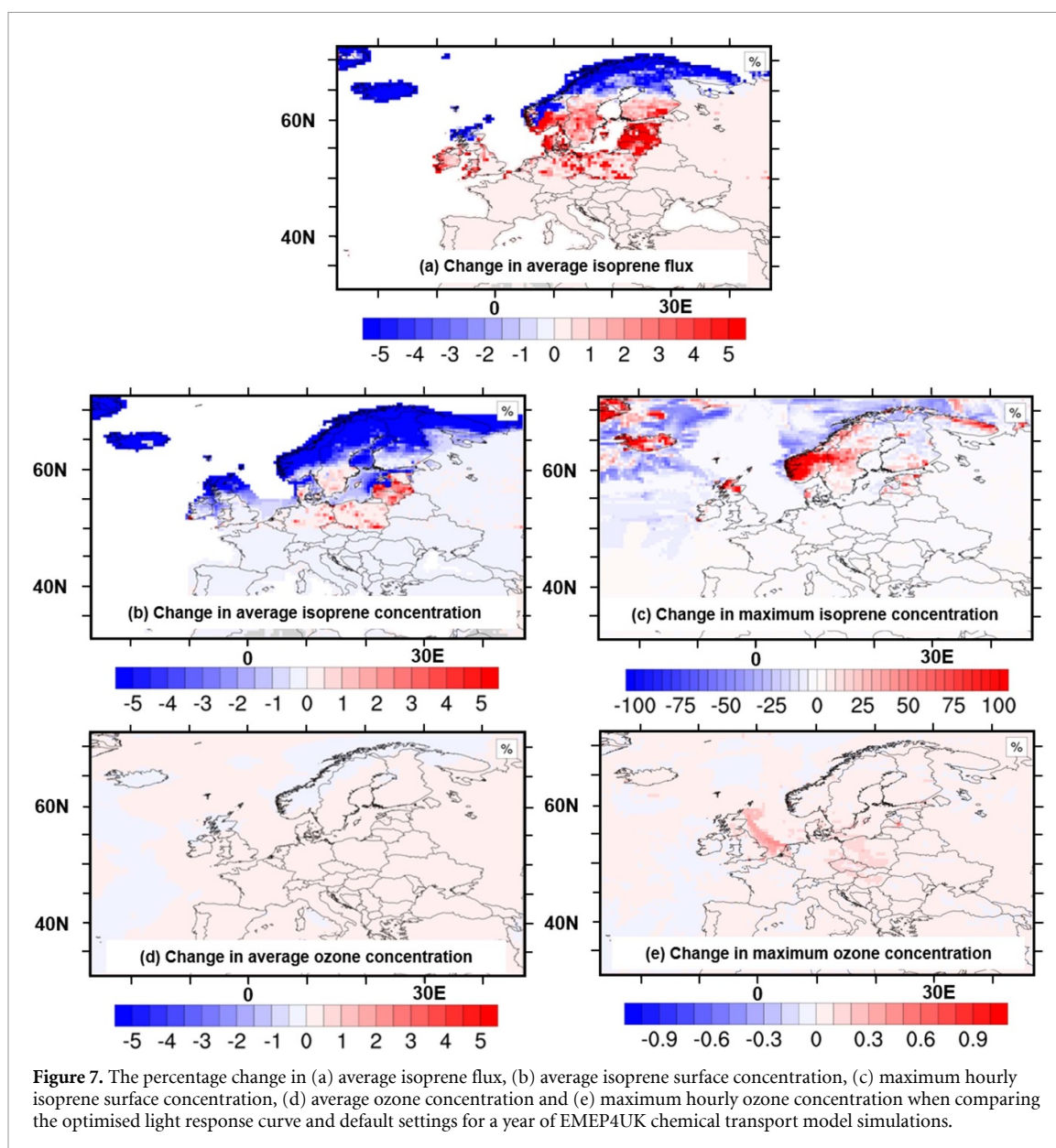
Figure 6. Frequency distributions of hourly isoprene emissions predicted for the Auchencorth Moss site in 2015 using the G93 emission algorithm with standard (purple) and optimised (pink) light response curves. Panel (a) shows the frequency distributions of predicted fluxes when using meteorological parameters measured at the Auchencorth Moss site and panel (b) shows frequency distributions of predicted fluxes derived using the EMEP4UK model meteorology.

3.4. Frequency distributions of modelled emissions

Isoprene emissions were simulated using both the standard and optimised light response curve driven by a full year of observed meteorology from the Auchencorth Moss site. The emissions were then simulated a second time using the EMEP4UK meteorology for the same year. Figure 6 shows the frequency distribution of the four emission simulations. When using the canopy-scale light response curve optimised for this specific site, the model yielded an average hourly emission rate of 19.9 μg m^{-2} h^{-1}. This was ~10% lower than when using the standard light response curve. The frequency distributions of emission rates shown in figure 6(a), show that although the optimised algorithm predicts more extreme values (>200 μg m^{-2} h^{-1}) than the standard algorithm, there are fewer emissions in the 100–200 μg m^{-2} h^{-1} range, resulting in a net reduction in total emissions over the full year. However, when using this optimised light response curve in conjunction with the simulated meteorology (WRF v3.7.1) used to drive the EMEP4UK model, the average emission was 23 μg m^{-2} h^{-1}, compared to 20 μg m^{-2} h^{-1} when using the standard light response. Figure 6(b) shows that the WRF meteorology reproduces the frequency distribution of temperature at our site reasonably well, but it overestimates the occurrence of summer clear sky conditions (figure 6(c)), resulting in a net increase in isoprene emissions compared to when using the standard light response. This suggests that whilst the physiologically specific light response curves for bryophytes can better represent emissions, the improvements are small relative to the uncertainties arising from the simulated meteorology.

3.5. Impact of moorland vegetation isoprene emissions on air quality

The revised light response curve was incorporated into the EMEP4UK model and applied to all moorland areas in the model domain north of a latitude of 50°. The isoprene emission potential was increased from the value 769 μg m^{-2} h^{-1} derived from Auchencorth Moss for the standard algorithm to 1035 μg m^{-2} h^{-1} which was the optimal value for the revised parameterisation. All other land-cover types were unchanged, using their default light response and isoprene emission potentials. The model was run for 2015 with the domain covering the whole of Europe. The results were compared to a base run, where default parameters were used, apart from the isoprene emission potential for moorland, which was set to 769 μg m^{-2} h^{-1} which

Figure 7. The percentage change in (a) average isoprene flux, (b) average isoprene surface concentration, (c) maximum hourly isoprene surface concentration, (d) average ozone concentration and (e) maximum hourly ozone concentration when comparing the optimised light response curve and default settings for a year of EMEP4UK chemical transport model simulations.

best described emissions at Auchencorth Moss based on the standard light response. Thus, the difference between the scenario calculation and the base run reflect the shape of the light response only, applied to all moorland vegetation north of 50°.

Figure 7(a) shows the percentage change in the average isoprene emissions when using the revised light parameterisation. In line with model simulations at Auchencorth Moss, the average annual isoprene emission rate is reduced while peak emissions increase by a factor of two (not shown). At latitudes below 55° north, there is a small increase in the average isoprene emission rate, which likely reflects a higher frequency of clear sky conditions.

The overall reduction in isoprene emission results in a corresponding reduction in average surface concentrations (figure 7(b)). Peak isoprene concentrations increase by up to a factor of two (figure 7(c)), but no significant changes in either the average surface ozone concentration (figure 7(e)) or maximum ozone concentrations (figure 7(f)) are evident. The low sensitivity of ozone to changing isoprene emissions indicates that the northern latitudes are strongly NO_x limited, with most semi-natural vegetation in the northern latitudes spatially segregated from the major NO_x sources found in the urban environment. This is partly due to the spatial segregation between NO_x emissions (around urban and industrial centres as well as along major roads) and semi-natural vegetation (away from populated areas), a well-established characteristic of the UK landscape (e.g. [46]).

Under a warming climate, isoprene emissions from the northern latitudes are expected to increase [47–49]. However, if the NO_x levels do not increase beyond present-day levels, these rises are unlikely to

contribute towards ozone related air quality issues in the future. Conversely, the role increased isoprene emissions may have on secondary organic aerosol (SOA) formation is less certain. On the one hand, increases in isoprene are likely to be outweighed by an associated increase of SOA precursors released from the boreal forest in the form of monoterpenes, which have a much higher SOA forming potential than that of isoprene. Yet, there is emerging evidence that isoprene emissions may actually help to supress the SOA yields from monoterpenes [50].

Further north, in the arctic tundra region, isoprene emissions, including those from bryophytes, constitute a greater proportion of the total biogenic VOC emissions and the ratio of isoprene to monoterpene emissions is predicted to increase with warming [47]. Therefore, emissions from these higher latitudes are likely to have a greater influence on new particle formation. Understanding the complex role of isoprene in mediating in SOA formation should now form a focus of future measurement and modelling efforts.

4. Conclusions

Eddy covariance fluxes were made above a Scottish ombrotrophic peatbog and revealed the ecosystem-scale emission potential to be comparable to that observed above a mixed oak forest in Italy [40]. Laboratory cuvette measurements attributed the source of these emissions to three moss species, *P. strictum, P. commune* and *S. fallax,* with additional, but unconfirmed emissions from *C. vulgaris* also likely to contribute to the observed fluxes. The whole-plant light response curves of isoprene emissions from these species did not follow the classical saturating curves observed in vascular plants and, therefore, the emissions from this site were poorly represented by the Guenther emission algorithms. Canopy-scale flux measurements of isoprene showed no sign of light saturation within the observed range (0–1800 μmol m^{-2} s^{-1} PAR), which meant the Guenther algorithms tended to over-predict emissions at lower PAR fluxes (<1000 μmol m^{-2} s^{-1}) and underestimate emissions under clear sky conditions (>1000 μmol m^{-2} s^{-1} PAR). The likely reason was that the light penetration curve for mosses differs significantly from that for other canopies. Although some emissions from grass or other vascular plant species at the site could not be ruled out, the general agreement between the light-response curves observed for moss under controlled conditions and the full ecosystem under ambient conditions suggests that such contributions would be minor.

Using the observations of flux measurements from this peatbog the light response curve was optimised to give the best fit to the observed emissions. When this new light response curve was incorporated into the EMEP4UK chemical transport model and extrapolated to all moorland within Europe, model predictions of the average annual isoprene emissions in the northern latitudes were reduced by >5%. The model was better able to capture peak emission rates at higher light intensities resulting in a significant increase in peak isoprene emissions. Despite a corresponding increase in peak isoprene concentrations by up to a factor of two, surface ozone concentrations were largely unaffected suggesting that in the northern latitudes, where this ecosystem type is dominant, photochemical ozone formation is strongly NO$_x$ limited due to the spatial segregation between biogenic isoprene emissions and NO$_x$ emissions from the urban environment. As such, the predicted increases in isoprene emissions from global warming are unlikely to contribute to ozone air quality issues provided that emissions of NO$_x$ do not go beyond their current levels.

Data availability statement

The data that support the findings of this study are openly available at the following DOI: https://doi.org/10.5285/f78b0f29-3df4-4a6c-a096-a1c73828b0a0.

Acknowledgments

ORCID iDs

Ben Langford ● https://orcid.org/0000-0002-6968-5197
James M Cash ● https://orcid.org/0000-0002-8567-1377
Massimo Vieno ● https://orcid.org/0000-0001-7741-9377
Mathew R Heal ● https://orcid.org/0000-0001-5539-7293

Julia Drewer ⓘ https://orcid.org/0000-0002-6263-6341
Christine F Braban ⓘ https://orcid.org/0000-0003-4275-0152
Eiko Nemitz ⓘ https://orcid.org/0000-0002-1765-6298

References

[1] Hanson D T, Swanson S, Graham L E and Sharkey T D 1999 Evolutionary significance of isoprene emission from mosses *Am. J. Bot.* **86** 634–9

[2] Atkinson R 2000 Atmospheric chemistry of VOCs and NO_x *Atmos. Environ.* **34** 2063–101

[3] Sillman S 1999 The relation between ozone, NO_x and hydrocarbons in urban and polluted rural environments *Atmos. Environ.* **33** 1821–45

[4] Emberson L 2020 Effects of ozone on agriculture, forests and grasslands *Phil. Trans. R. Soc.* A **378** 20190327

[5] Screpanti A and de Marco A 2009 Corrosion on cultural heritage buildings in Italy: a role for ozone? *Environ. Pollut.* **157** 1513–20

[6] Lippmann M 1991 Health effects of tropospheric ozone *Environ. Sci. Technol.* **25** 1954–62

[7] Claeys M *et al* 2004 Formation of secondary organic aerosols through photooxidation of isoprene *Science* **303** 1173–6

[8] Janson R and de Serves C 1998 Isoprene emissions from boreal wetlands in Scandinavia *J. Geophys. Res.* **103** 25513–7

[9] Faubert P, Tiiva P, Rinnan Å, Räsänen J, Holopainen J K, Holopainen T, Kyrö E and Rinnan R 2010 Non-methane biogenic volatile organic compound emissions from a subarctic peatland under enhanced UV-B radiation *Ecosystems* **13** 860–73

[10] Lindwall F, Faubert P and Rinnan R 2015 Diel variation of biogenic volatile organic compound emissions—a field study in the sub, low and high arctic on the effect of temperature and light *PLoS One* **10** e0123610

[11] Rinnan R, Saarnio S, Haapala J K, Mörsky S K, Martikainen P J, Silvola J and Holopainen T 2013 Boreal peatland ecosystems under enhanced UV-B radiation and elevated tropospheric ozone concentration *Environ. Exp. Bot.* **90** 43–52

[12] Tiiva P, Rinnan R, Faubert P, Räsänen J, Holopainen T, Kyrö E and Holopainen J K 2007 Isoprene emission from a subarctic peatland under enhanced UV-B radiation *New Phytol.* **176** 346–55

[13] Ekberg A, Arneth A and Holst T 2011 Isoprene emission from *Sphagnum* species occupying different growth positions above the water table *Boreal Environ. Res.* **16** 47–59

[14] Haapanala S, Rinne J, Pystynen K-H, Hellén H, Hakola H and Riutta T 2006 Measurements of hydrocarbon emissions from a boreal fen using the REA technique *Biogeosciences* **3** 103–12

[15] Kramshøj M, Vedel-Petersen I, Schollert M, Rinnan Å, Nymand J, Ro-Poulsen H and Rinnan R 2016 Large increases in Arctic biogenic volatile emissions are a direct effect of warming *Nat. Geosci.* **9** 349–52

[16] Arneth A *et al* 2007 Process-based estimates of terrestrial ecosystem isoprene emissions: incorporating the effects of a direct CO_2-isoprene interaction *Atmos. Chem. Phys.* **7** 31–53

[17] Niinemets Ü, Tenhunen J D, Harley P C and Steinbrecher R 1999 A model of isoprene emission based on energetic requirements for isoprene synthesis and leaf photosynthetic properties for *Liquidambar* and *Quercus Plant Cell. Environ.* **22** 1319–35

[18] Guenther A B, Zimmerman P R, Harley P C, Monson R K and Fall R 1993 Isoprene and monoterpene emission rate variability—model evaluations and sensitivity analyses *J. Geophys. Res.* **98** 12609–17

[19] Guenther A *et al* 1995 A global-model of natural volatile organic-compound emissions *J. Geophys. Res.* **100** 8873–92

[20] Guenther A, Karl T, Harley P, Wiedinmyer C, Palmer P I and Geron C 2006 Estimates of global terrestrial isoprene emissions using MEGAN (model of emissions of gases and aerosols from nature) *Atmos. Chem. Phys.* **6** 3181–210

[21] Guenther A B, Jiang X, Heald C L, Sakulyanontvittaya T, Duhl T, Emmons L K and Wang X 2012 The model of emissions of gases and aerosols from nature version 2.1 (MEGAN2.1): an extended and updated framework for modeling biogenic emissions *Geosci. Model. Dev.* **5** 1471–92

[22] Roberts A, Roberts E and Haigler C 2012 Moss cell walls: structure and biosynthesis *Front. Plant Sci.* **3** 166

[23] Deakova T 2019 Isoprene emission in polytrichaceae mosses *Dissertations and Theses* Portland State University

[24] Billett M F, Palmer S M, Hope D, Deacon C, Storeton-West R, Hargreaves K J, Flechard C and Fowler D 2004 Linking land-atmosphere-stream carbon fluxes in a lowland peatland system *Glob. Biogeochem. Cycles* **18** GB1024

[25] Drewer J *et al* 2010 Comparison of greenhouse gas fluxes and nitrogen budgets from an ombrotrophic bog in Scotland and a minerotrophic sedge fen in Finland *Eur. J. Soil Sci.* **61** 640–50

[26] Dinsmore K J, Skiba U M, Billett M F, Rees R M and Drewer J 2009 Spatial and temporal variability in CH_4 and N_2O fluxes from a Scottish ombrotrophic peatland: implications for modelling and up-scaling *Soil Biol. Biochem.* **41** 1315–23

[27] Langford B, Nemitz E, House E, Phillips G J, Famulari D, Davison B, Hopkins J R, Lewis A C and Hewitt C N 2010 Fluxes and concentrations of volatile organic compounds above central London, UK *Atmos. Chem. Phys.* **10** 627–45

[28] Langford B, Acton W, Ammann C, Valach A and Nemitz E 2015 Eddy-covariance data with low signal-to-noise ratio: time-lag determination, uncertainties and limit of detection *Atmos. Meas. Tech.* **8** 4197–213

[29] Langford B *et al* 2022 Isoprene concentration and flux measurements and associated meteorological parameters from Auchencorth Moss, Scotland, June and July, 2015 (NERC EDS Environmental Information Data Centre)

[30] Hanson D T and Sharkey T D 2001 Rate of acclimation of the capacity for isoprene emission in response to light and temperature Plant, Cell & Environment **24** 937–46

[31] Rasulov B, Hüve K, Bichele I, Laisk A and Niinemets Ü 2010 Temperature response of isoprene emission *in vivo* reflects a combined effect of substrate limitations and isoprene synthase activity: a kinetic analysis *Plant Physiol.* **154** 1558–70

[32] Csiky O and Seufert G 1999 Terpenoid emissions of Mediterranean oaks and their relation to taxonomy *Ecol. Appl.* **9** 1138–46

[33] Guenther A B, Monson R K and Fall R 1991 Isoprene and monoterpene emission rate variability—observations with eucalyptus and emission rate algorithm development *J. Geophys. Res.* **96** 10799–808

[34] Simpson D *et al* 2012 The EMEP MSC-W chemical transport model—technical description *Atmos. Chem. Phys.* **12** 7825–65

[35] Skamarock W C *et al* 2019 A description of the advanced research WRF version 4 (NCAR) p 145

[36] Vieno M *et al* 2014 The role of long-range transport and domestic emissions in determining atmospheric secondary inorganic particle concentrations across the UK *Atmos. Chem. Phys.* **14** 8435–47

[37] Vieno M, Heal M R, Williams M L, Carnell E J, Nemitz E, Stedman J R and Reis S 2016 The sensitivities of emissions reductions for the mitigation of UK $PM_{2.5}$ *Atmos. Chem. Phys.* **16** 265–76

[38] Ge Y, Heal M R, Stevenson D S, Wind P and Vieno M 2021 Evaluation of global EMEP MSC-W (rv4.34) WRF (v3.9.1.1) model surface concentrations and wet deposition of reactive N and S with measurements *Geosci. Model Dev.* **14** 7021–46

[39] Guenther A, Zimmerman P and Wildermuth M 1994 Natural volatile organic compound emission rate estimates for U.S. woodland landscapes *Atmos. Environ.* **28** 1197–210

[40] Langford B *et al* 2017 Isoprene emission potentials from European oak forests derived from canopy flux measurements: an assessment of uncertainties and inter-algorithm variability *Biogeosciences* **14** 5571–94

[41] Murray K J, Tenhunen J D and Nowak R S 1993 Photoinhibition as a control on photosynthesis and production of *Sphagnum* mosses *Oecologia* **96** 200–7

[42] Langford B, Misztal P K, Nemitz E, Davison B, Helfter C, Pugh T A M, MacKenzie A R, Lim S F and Hewitt C N 2010 Fluxes and concentrations of volatile organic compounds from a South-East Asian tropical rainforest *Atmos. Chem. Phys.* **10** 8391–412

[43] Langford B *et al* 2022 Seasonality of isoprene emissions and oxidation products above the remote Amazon *Environ. Sci. Atmos.* **2** 230–40

[44] Marschall M and Proctor M C F 2004 Are bryophytes shade plants? Photosynthetic light responses and proportions of chlorophyll a, chlorophyll b and total carotenoids *Ann. Bot.* **94** 593–603

[45] Perera-Castro A V *et al* 2020 It is hot in the sun: Antarctic mosses have high temperature optima for photosynthesis despite cold climate *Front. Plant Sci.* **11** 1178

[46] Group A Q E 2021 Ozone in the UK—recent trends and future projections 1–143

[47] Rinnan R, Iversen L L, Tang J, Vedel-Petersen I, Schollert M and Schurgers G 2020 Separating direct and indirect effects of rising temperatures on biogenic volatile emissions in the Arctic *Proc. Natl Acad. Sci. USA* **117** 32476–83

[48] Lindwall F, Schollert M, Michelsen A, Blok D and Rinnan R 2016 Fourfold higher tundra volatile emissions due to arctic summer warming *J. Geophys. Res.* **121** 895–902

[49] Potosnak M J, Baker B M, LeStourgeon L, Disher S M, Griffin K L, Bret-Harte M S and Starr G 2013 Isoprene emissions from a tundra ecosystem *Biogeosciences* **10** 871–89

[50] McFiggans G *et al* 2019 Secondary organic aerosol reduced by mixture of atmospheric vapours *Nature* **565** 587–93